Mechanism for electron emission and exciton formation during collisions of neutral hydrogens with a LiF(001) surface

J. E. Miraglia

Instituto de Astronomía y Física del Espacio, Consejo Nacional de Investigaciones Científicas y Técnicas, and Departamento de Física, Facultad de Ciencias Exactas y Naturales, Universidad de Buenos Aires, Casilla de Correo 67, Sucursal 28, C1428EGA Buenos Aires, Argentina

(Received 19 September 2014; published 31 December 2014)

In this article we propose an unexplored mechanism to understand the physics underlying the electron emission and exciton formation occurring during grazing impact of neutral hydrogen atoms on LiF(100) surfaces. Instead of adopting the traditional point of view considering the negative ion formation as the precursor of the processes, we investigate the formation of excited hydrogen H($n = 2$) as a catalyzer to produce excitons and electrons. We base our proposal on *ab initio* calculations that compare quite well with experiments for impact energies larger than 4 keV.

DOI: 10.1103/PhysRevA.90.062715 PACS number(s): 79.20.Rf, 73.20.Mf, 34.50.Fa

I. INTRODUCTION

In recent years considerable progress has been achieved in the understanding of fast atom diffraction (FAD) occurring under axial channeling conditions [1–5]. Here scattered projectile distributions display well-defined diffraction patterns originated from the periodic structure of the crystal. A recent article experimentally studied the *decoherence* of FAD patterns for neutral keV hydrogen and helium atoms from a LiF(001) surface [6]. For hydrogen atoms, the authors found that electron excitations and excitons of the target surface were the dominant mechanisms of decoherence, whereas for helium impact these contributions were negligibly small. This places the neutral hydrogen in a particular situation with respect to the LiF electronic structure, and this is what we investigate in this work.

We deal with inelastic processes, namely electron emission and exciton formation, occurring during scattering of neutral hydrogen atoms from a LiF(001) surface under planar conditions: this is at a random azimuthal orientation. There have been a good deal of experiments relevant to this subject in the last 20 years [7–9]. By relating the energy loss spectra with the number of emitted electrons, the experimental data were interpreted in terms of the formation of negative hydrogen as a precursor for electron excitation and emission. This negative ion is expected to come about in the vicinities of the negative fluorine ion, which is considered the active site. Fitting the data considering three basic processes—binary, Landau-Zener, and detachment; inserting the corresponding probabilities in the binomial distribution; and considering 12 collisions independent of the impact parameter—the resulting statistics reproduces quite well the experiments. The impact energies investigated ranged from 600 eV [7] to 10 keV [8]. The formation of negative oxygen and fluorine ions was also experimentally found in high proportions when impacting the corresponding neutral atoms on a LiF(100) surface [10,11]. The data showed a maximum of H^- fractions of 7% around 2.5 keV, while O^- and F^- fractions were measured to be up to ten times larger [11].

In the present article we put forward an alternative mechanism to explain the data based in the formation of hydrogen excited states, valid only for impact energies larger than 5 keV. We present detailed calculations that prove that H($n = 2$) is an important channel—though not the only one—determining the number of inelastic transitions. Our scheme can be synthesized as follows: besides the direct transitions, the incident H($1s$) can be excited to H($n = 2$), mainly at the Li^+ sites. In the next collisions the fate of H($n = 2$) atoms bifurcates; they can either be ionized and so contribute to electron emission or they can produce an exciton via transfer excitation. In the former case, the remaining proton should capture an electron to continue its routine with efficiency depending on the impact parameter. In this way the excited hydrogen atom becomes a catalyzer of the inelastic processes. With this mechanism we can explain the data for energies higher than 5 keV, whereas for lower energies the formation of H^- remains the only possible mechanism.

The article is organized as follows. In Sec. II we summarize the theoretical treatment and the details of the calculation. In Sec. III we present the results and in Sec. IV we compare them with the experiments. Conclusions are left to Sec. V. Atomic units are used unless otherwise stated.

II. THE THEORETICAL TREATMENT

As mentioned in the introduction we concentrate on the inelastic processes occurring during the impact of neutral hydrogen H($1s$) on a LiF(001) surface. By inelastic channels we mean electron emission and exciton production, which in terms of our atomic description can be understood as ionization and electron excitation of the target. At the impact energies relevant to the experiments, there is no simple theory to apply, but we can exploit the fact that the experiments were performed under grazing incidence. This means that the collision takes place at large distances, i.e., at some atomic units from the surface, which makes it possible to use just the first perturbative order. In synthesis we have proceeded as follows.

We start treating an individual electronic transition within the independent electron model, considered as a simple atomic collision between a projectile and a crystal site. Each transition involves only one active electron in the target or in the projectile which suffers the excitation or ionization. The ten electrons of the F^- site are described by a full Hartree-Fock wave function of the many-electron system in

a central potential given by $-10/r + V_M^-(\rho,r)$, where V_M^- is the Madelung potential [12],

$$V_M^-(\rho,r) = -\frac{1}{r} + \frac{e^{-r/\rho}}{r}\left[1 + (1-\rho V_{M\infty})\frac{r}{\rho} + \left(\frac{1}{2} - \rho V_{M0}\right)\left(\frac{r}{\rho}\right)^2\right] \to \begin{cases} -V_{M0}, & r \to 0 \\ -\frac{1}{r}, & r \to \infty \end{cases}, \quad (1)$$

with $\rho = 0.14$. In Eq. (1), $V_{M0} = 0.4600$ a.u. $= 12.51$ eV is the Madelung binding value. Chemical properties, binding energies, mean radios, etc. are published elsewhere [13]. Similarly, the two electrons of the Li^+ site are also described by the Hartree-Fock function in a central potential given by $-3/r - V_M^-(\rho,r)$. We denote these two-dressed ions as $F_@^-$ and $Li_@^+$. Electron bound states of the projectile are simply hydrogenic.

The calculation was performed in first Born approximation, which is fully numerically evaluated. It means that we use initial and final numerical wave functions for the effective potentials given in Ref. [13]. In the case of ionization, we use an expansion of the continuum state in spherical harmonics, evaluating the transition matrix $T_{fi}(\vec{\eta})$ in a grid of emitted electron energies E, angles θ, and transverse momentum $\vec{\eta}$. Details of the calculation are given in Ref. [14].

Next we employ the usual eikonal approximation to calculate the probability of transition as a function of the impact parameter $P_{fi}(\vec{b})$:

$$P_{fi}(\vec{b}) = \left| \int \frac{d\vec{\eta}}{2\pi} \exp(i\vec{\eta}\cdot\vec{b})\, T_{fi}(\vec{\eta}) \right|^2. \quad (2)$$

A careful inspection of $P_{fi}(\vec{b})$ is very important to check that we are indeed in the perturbative regime. In all the cases studied here we introduced a minimum impact parameter, $b_{\min} = 2.5$ a.u., which is the sum of mean radii of $F_@^-(2p)$ and $H(1s)$, requiring that

$$P_{fi}(b_{\min}) \lesssim 0.01, \quad (3)$$

to warrant a perturbative regime where the first Born approximation holds. Recall that we are dealing with direct transitions, i.e., ionization and excitation, where the Born approximation is expected to describe the limit of large distances.

Knowing $P_{fi}(b)$ we can calculate the probability of transition as a function of the distance to the topmost hosting surface where the ion is located, $W_{fi}(Z)$:

$$W_{fi}(Z) = 2\int_Z^\infty \frac{db\, b}{\sqrt{b^2 - Z^2}} P_{fi}(b). \quad (4)$$

The total cross section per atom is then expressed as

$$\sigma_{fi} = \int_{-\infty}^{\infty} dZ\, W_{fi}(Z) = 2\pi \int_0^\infty db\, b P_{fi}(b). \quad (5)$$

Under the planar incident condition, the projectile follows a classical trajectory determined by the interacting potential as a function of the distance to the surface, $V_i(Z)$ [5,13]. The number of $i \to f$ transitions is then given by

$$N_{fi} = 2\int_{Z_{\min}}^\infty dZ \frac{\delta_s v_i\, W_{fi}(Z)}{\sqrt{(v_i\theta_i)^2 - \frac{2}{M_P}V_i(Z)}}, \quad (6)$$

where v_i is the impact velocity of the projectile, M_P is its mass, θ_i is the incident angle with respect to the surface, and δ_s is the superficial density of targets. In Eq. (6) $Z_{\min}$ is the minimal distance satisfying $V_i(Z_{\min}) = 1/2M_P\,(v_i\theta_i)^2 = E_t$, where E_t is the experimental transverse energy. For the cases studied experimentally the transverse energy is $E_t \simeq 1$ eV, and for $H(1s)$ the turning point $Z_{\min}$ situates around 3.5 a.u. Probabilities at this point are small enough to be perturbative. In this way we calculate the number of emitted electrons $N_{\rm el}$ and excitons $N_{\rm ex}$ produced along the whole trajectory.

Knowing that $N = N_{\rm el/ex}$ is the average of the inelastic rate, then the probability of a given number of independent events in time n is given by the Poisson distribution [15]. Then the probability of producing n transitions is given by

$$p_n = \frac{N^n}{n!}e^{-N}, \quad (7)$$

which permits a direct comparison with the statistical data. We come back to this point.

III. RELEVANT MECHANISMS

In this section we review different mechanisms leading to electron and exciton productions. First, we note that experiments have shown that the results do not change significantly whether impacts are H^+ or $H(1s)$, which makes us assume that the proton neutralizes very rapidly. And this is expected since the neutralization reaction

$$H^+ + F_@^-(2p) \to H(1s) + F_@^0 \quad (8)$$

is quasiresonant; i.e., the binding energy of the ground state of hydrogen is very close to the binding energy of $F_@^-(2p)$. This is a consequence of the Madelung potential at the origin V_{M0} that shifts down the binding energy.

Second, we note that indeed the impinging of $H(1s)$ cannot explain alone the experiments. In Figs. 1(a) and 1(b) we display the number of inelastic transitions, $N_{{\rm elH}(1s)}$ and $N_{{\rm exH}(1s)}$, calculated with Eq. (6) for the two direct cases, respectively:

$$H(1s) + F_@^-(2p) \to H(1s) + F_@^0 + e, \quad (9)$$

$$H(1s) + F_@^-(2p) \to H(1s) + F_@^-(n=3), \quad (10)$$

The value $N_{{\rm elH}(1s)}$ gives the number of emitted electrons, while $N_{{\rm exH}(1s)}$ gives the number of excitons, $2p \to n = 3 = 3s + 3p_{0\pm1} + 3d_{0\pm1\pm2}$. The figure displays the dependencies of both magnitudes with the angle of incidence θ_i for different impact energies, as indicated. It is also shown in the figure the values correspond to the transverse energy $E_t = 1$ eV. This is the case studied in Ref. [8], which is considered a benchmark. The inelastic channels given by Eqs. (9) and (10) cannot fully explain the experimental data. For ionization at 5 keV impact energy, we have $N_{{\rm elH}(1s)} = 0.4$ electrons and $N_{{\rm exH}(1s)} = 0.5$ excitons while the experiment gives around 7 and 3, respectively.

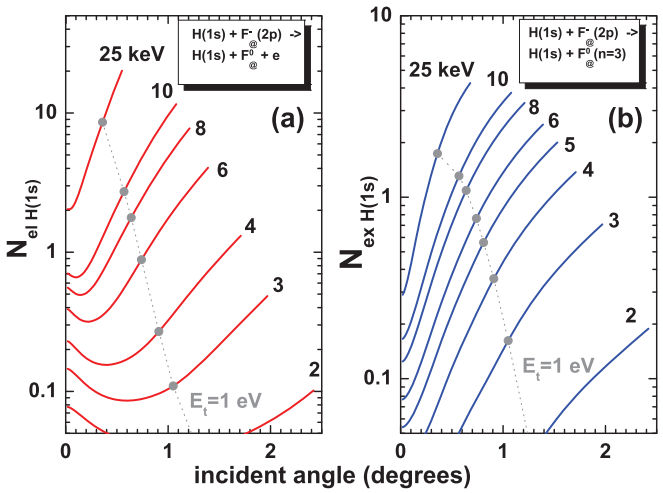

FIG. 1. (Color online) Calculated number of target (a) electrons, $N_{\rm el}$, and (b) excitons, $N_{\rm ex}$, produced by the impact of H(1s) on LiF(001) as a function of the incident angle θ_i for different impact energies as indicated. Symbols connected with a dotted line correspond to the values where the transversal energy is 1 eV.

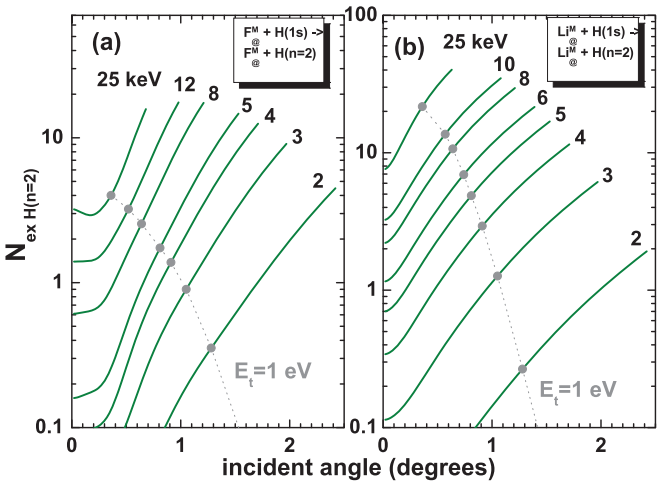

FIG. 2. (Color online) Calculated number of projectile excitations $N_{\rm ex}$ to H($n=2$) ($nl=2s+2p_{0\pm1}$) produced by the impact of (a) $F^M_@$ and (b) $Li^M_@$ on H(1s), as a function of the incident angle θ_i for different impact energies as indicated. Symbols connected with a dotted line correspond to the values where the transversal energy is 1 eV.

To explain the experimental data, our proposition is based on the contribution of the projectile excitation channel which could play the role of a catalyzer for both inelastic transitions, namely,

$$\mathrm{H}(1s)+\begin{pmatrix}\mathrm{F}^M_@\\ \mathrm{Li}^M_@\end{pmatrix}\rightarrow \mathrm{H}(n=2)+\begin{pmatrix}\mathrm{F}^M_@\\ \mathrm{Li}^M_@\end{pmatrix}, \tag{11}$$

where with $F^M_@$ and $Li^M_@$ we denote the target sites involved in the excitation process. We have to be very careful about the strength of the surface sites. In principle the static potential between the *individual* crystal sites and the projectile electron are asymptotically Coulombic:

$$V_{\mathrm{F}^-_@}(r)=-\frac{9}{r}+\int d\vec{r}\,'\frac{n_{\mathrm{F}^-_@}(\vec{r}\,')}{|\vec{r}\,'-\vec{r}\,|}\underset{r\rightarrow\infty}{\rightarrow}+\frac{1}{r}, \tag{12}$$

$$V_{\mathrm{Li}^+_@}(r)=-\frac{3}{r}+\int d\vec{r}\,'\frac{n_{\mathrm{Li}^+_@}(\vec{r}\,')}{|\vec{r}\,'-\vec{r}\,|}\underset{r\rightarrow\infty}{\rightarrow}-\frac{1}{r}. \tag{13}$$

But as the projectile separates from the surface the binary Coulombic interaction starts to be affected by the neighboring contributions that eventually cancel it. To be consistent with the calculation of the wave function, we approximate the effect of the neighbors by considering the Madelung potentials V_M. The potentials then reduce to

$$V_{\mathrm{F}^M_@}(r)=V_{\mathrm{F}^-_@}(r)+V_M\underset{r\rightarrow\infty}{\rightarrow}+\frac{0}{r}, \tag{14}$$

$$V_{\mathrm{Li}^M_@}(r)=V_{\mathrm{Li}^-_@}(r)-V_M\underset{r\rightarrow\infty}{\rightarrow}+\frac{0}{r}. \tag{15}$$

In Figs. 2(a) and 2(b) we plot the number of projectile excited electrons to H($nl=2s+2p_{0\pm1}$) $N_{\mathrm{exH}(n=2)}$ using $V_{\mathrm{F}^M_@}$ and $V_{\mathrm{Li}^M_@}$ as excitation promoters. It can be observed that several excitations can take place, especially coming from $Li^+_@$ sites. And this is to be expected, because the $Li^+_@$ ratio is very small, and so $V_{\mathrm{Li}^-_@}$ remains fully Coulombic until V_M starts to cancel it according to Eq. (15). On the other hand, $V_{\mathrm{F}^-_@}$ tends to a Coulombic behavior, very slowly passing through a point that is neutral. In fact it never reaches its pure Coulombic form because V_M cancels it beforehand.

The formation of H($n=2$) can contribute to the other electron or excitation production via collisions with another crystal site:

$$\mathrm{H}(n=2)+\begin{pmatrix}\mathrm{F}^M_@\\ \mathrm{Li}^M_@\end{pmatrix}\rightarrow \mathrm{H}^+ + e+\begin{pmatrix}\mathrm{F}^M_@\\ \mathrm{Li}^M_@\end{pmatrix}, \tag{16}$$

$$\mathrm{H}(n=2)+\mathrm{F}^-_@(2p)\rightarrow \mathrm{H}(1s)+\mathrm{F}^-_@(3s). \tag{17}$$

The reaction given by Eq. (16) contributes to the electron emission. In this case, the residual proton is expected to neutralize rapidly to start the process again, and so to play the role of catalyzer. We call attention to the transfer excitation given by Eq. (17). This two-electron transition is expected to be very active because it represents an almost resonant process: the electron projectile energy $\Delta_{\rm H}=\varepsilon_{\rm H}(n=2)-\varepsilon_{\rm H}(1s)=10.2$ eV is very close to the target one, $\Delta_{\mathrm{F}^-_@}=\varepsilon_{\mathrm{F}^-_@}(n=2)-\varepsilon_{\mathrm{F}^-_@}(1s)=10.7$ eV. In both reactions given by Eqs. (16) and (17), the projectile returns to H(1s) to continue its job. Again, at 5 keV H(1s) impact, it could produce up to 6.6 electrons or excitons depending on the bifurcation ratio, and this is a determinant magnitude considering that the experiment gives about 7 electrons per projectile.

The intermediate channel H($n=2$) is not the only one to take into account; there are other possible reactions which are neither decisive nor negligible. For example, let us take the number of excitation to H($n=3$), $N_{\mathrm{exH}(n=3)}$:

$$\mathrm{H}(1s)+\begin{pmatrix}\mathrm{F}^M_@\\ \mathrm{Li}^M_@\end{pmatrix}\rightarrow \mathrm{H}(n=3)+\begin{pmatrix}\mathrm{F}^M_@\\ \mathrm{Li}^M_@\end{pmatrix}, \tag{18}$$

as plotted in Figs. 3(a) and 3(b). As the electron in H($n=3$) is loosely bound, this intermediate channel certainly contributes

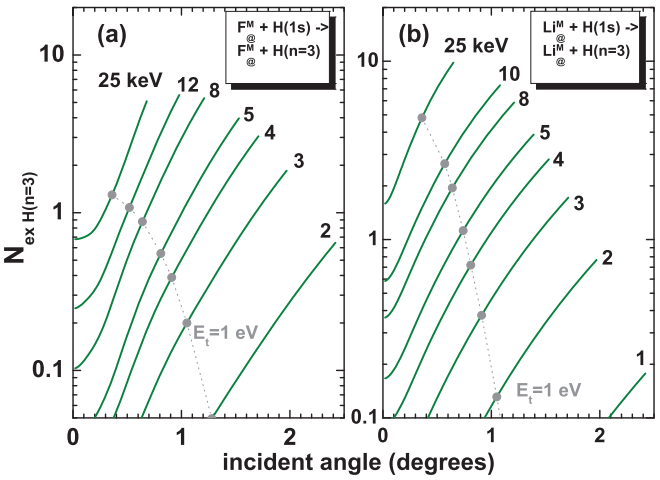

FIG. 3. (Color online) Calculated number of projectile excitations to H($n = 3$) ($nl = 3s + 3p_{0\pm1} + 3d_{0\pm1\pm2}$) produced by the impact of (a) $F^M_@$ and (b) $Li^M_@$ on H($1s$) as a function of the incident angle θ_i for different impact energies as indicated. Symbols connected with dotted line correspond to the values where the transversal energy is 1 eV.

mostly to electron production via collisions with other crystal sites, schematically

$$\mathrm{H}(n=3) + \begin{pmatrix} \mathrm{F}^M_@ \\ \mathrm{Li}^M_@ \end{pmatrix} \rightarrow \mathrm{H}^+ + e + \begin{pmatrix} \mathrm{F}^M_@ \\ \mathrm{Li}^M_@ \end{pmatrix}. \qquad (19)$$

IV. COMPARISON WITH THE EXPERIMENTS

In Figure 4(a) we show the contribution of the different channels to exciton and electron formation along with the experimental values for electron emission and number of excitons derived from the fitting model published in Ref. [8] for $E_t = 1$ eV. First, one can infer that for energies higher than 5 keV the experiments run approximately within the possible margin:

$$N_{\mathrm{elH}(1s)} \lesssim N_{\mathrm{el}} \lesssim N_{\mathrm{elH}(1s)} + N_{\mathrm{exH}(n=2)} + N_{\mathrm{exH}(n=3)}, \qquad (20)$$

$$N_{\mathrm{exH}(1s)} \lesssim N_{\mathrm{ex}} \lesssim N_{\mathrm{exH}(1s)} + N_{\mathrm{exH}(n=2)}, \qquad (21)$$

where we have considered that $N_{\mathrm{exH}(n=3)}$ contributes only to electron production. As we do not know the bifurcation values of the excited projectile states H($n = 2$), it is convenient to add up all the inelastic contributions, $N^{\mathrm{tot}} = N_{\mathrm{el}} + N_{\mathrm{ex}}$:

$$N^{\mathrm{tot}} = N_{\mathrm{elH}(1s)} + N_{\mathrm{exH}(1s)} + N_{\mathrm{exH}(n=2)} + N_{\mathrm{exH}(n=3)}, \qquad (22)$$

as shown in Fig. 4(b), where we can see the good performance of our model compared with the experiments for impact energies in the range 5–10 keV. In consequence, to give space to our mechanism, we have to assume forcibly a reduction of the H^- production for energies larger than 5 keV.

Finally we concentrate on the statistics to support the Poisson distribution in place of the binomial one used in Ref. [9]. Let us take again 5 keV impact energy, where the number of electron statistics was measured and compared with the fitted binomial distribution (Fig. 8 of Ref. [9]). Considering a splitting of $N_{\mathrm{H}(n=2)}$ of 63% and 37% for electron and exciton

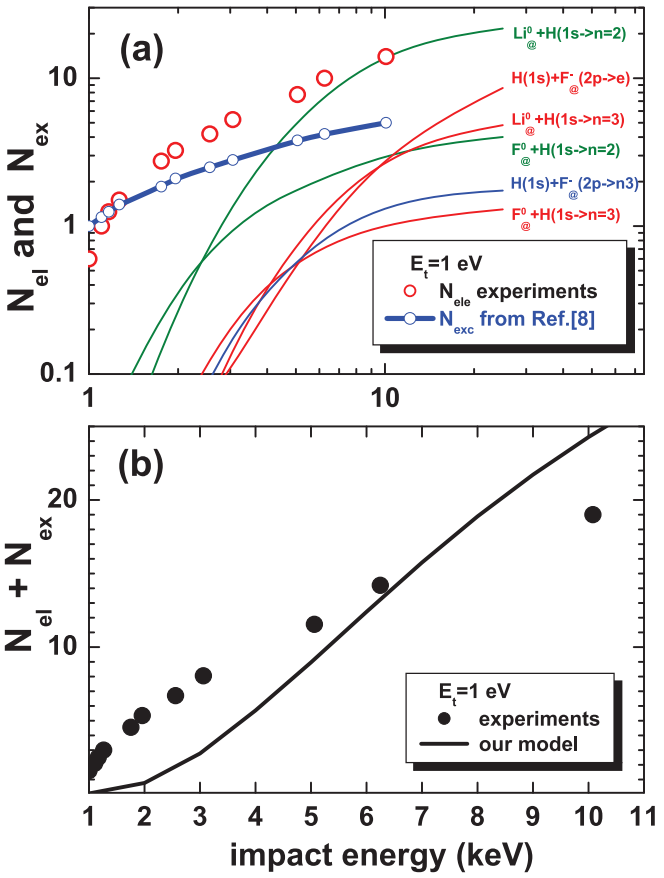

FIG. 4. (Color online) (a) Calculated number of electrons, N_{el}, and excitons, N_{ex}, as a function of the total impact energy for transversal energy $E_t = 1$ eV for different processes as indicated. Open symbols denote the experimental number of electrons; the thick line is the experimentally adjusted model for the number of excitations (Fig. 4 from Ref. [8]). (b) The solid line indicates total yields of inelastic transitions, $N_{\mathrm{el}} + N_{\mathrm{ex}}$, and the symbols correspond to the sum of the experimental values.

productions, respectively, we have

$$N_{\mathrm{el}} = 0.63N_{\mathrm{exH}(n=2)} + N_{\mathrm{elH}(1s)} + N_{\mathrm{H}(n=3)} \simeq 6, \qquad (23)$$

$$N_{\mathrm{ex}} = 0.37N_{\mathrm{exH}(n=2)} + N_{\mathrm{exH}(1s)} \simeq 3. \qquad (24)$$

A number of excitons $N_{\mathrm{ex}} = 3$ is in near agreement with the best-fit binomial distribution reported in Fig. 4 of Ref. [8]. The Poisson distribution given by Eq. (7) with $N_{\mathrm{el}} = 6$ is plotted in Fig. 5 and compared with the experiments. The agreement with the data is excellent.

Remarks

In what follows we want to briefly compile some limitations and remarks to be taken into account in future developments.

The values of N_{el} and N_{ex} are very sensitive to the turning point Z_{min} and in the end with the model to calculate the surface potential. A small decrease of Z_{min} is reflected in a significant increase of the values of N_{el} and N_{ex}.

We did not consider the change of the Madelung potential due to the surface. This effect moves up the binding energies

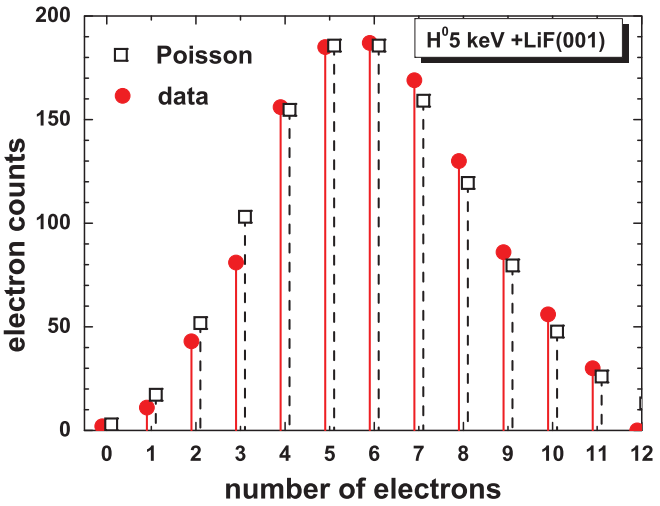

FIG. 5. (Color online) Bar graph of experimental electron number distribution (solid symbols) (from Fig. 8 of Ref. [9]) and compared with the Poisson distribution (open symbols) with $N_{\rm el} = 6$, for 5 keV H($1s$) impact on a LiF(001) surface at $\theta_i = 0.8^\circ$ ($E_t = 1$ eV).

about 0.5 eV. Nor have we consider the breadth of the band structure having a width at the base of 3.5 eV, lower with respect to the Γ point.

To proceed to lower energies (below 5 keV), we need to calculate the probability of negative hydrogen formation at the $F^-_@$ site:

$$\mathrm{H}(1s) + \mathrm{F}^-_@(2p) \rightarrow \mathrm{H}^-(1s^2) + \mathrm{F}^0_@. \qquad (25)$$

Its calculation requires, as reaction (17), a two-active-electron model.

To deal with a more general case in which we have cascades (large values of $N_{\rm el}$ and $N_{\rm ex}$), it is necessary to calculate the coupling between all the possible channels, which in the present cases is a considerable number, and resort to the master equation

$$\frac{dN_f}{dZ} = \sum_i \frac{\delta_s v_i \; W_{fi}(Z)\; N_i}{\sqrt{(v_i\theta_i)^2 - \frac{2}{M_P}V_i(Z)}} - \sum_l \frac{\delta_s v_i \; W_{lf}(Z)\; N_f}{\sqrt{(v_i\theta_i)^2 - \frac{2}{M_P}V_f(Z)}}. \qquad (26)$$

Equation (6) can be obtained from Eq. (26) in a first perturbative order. Anyway, as in ion-solid collisions, an advisable method to deal with this problem is the classical trajectory Monte Carlo method. In this case, the mean free path should be counted along the classical path consistent with the particular trajectory followed by the projectile state and charge under consideration.

As observed in Fig. 4, at the highest impact energies our simple model overestimates the experimental results. And the main reason is that we are using the simple Eq. (6) instead of the fully coupled Eq. (26). The full master equation allows other channels to come into existence. An example is capture after ionization, which has not been included here.

V. CONCLUSIONS

We have proposed a mechanism to understand the physics underlying the electron emission and exciton formation occurring during grazing collisions of neutral hydrogen on a LiF(001) surface. Instead of visualizing the negative ion formation as the precursor, we have considered the formation of excited H($n = 2$) as a catalyzer to produce excitons and electrons. The present mechanism is valid only for proton impact energies larger than 5 keV. We have built our interpretation with solid calculations. The very important point that we want to stress here is that our calculation holds on its own; it is a free-fitting parameters calculation. However, the entire physics is far from being fully understood, the formation of excited hydrogen cannot explain the whole situation, and other transitions can take place and contribute to the final result. The whole process seems to be complex, not only due to the large amount of calculations required but also to the sensibility of the approximation used.

ACKNOWLEDGMENTS

We wish to thank Raul Baragiola for encouraging this work. This work was partially supported by the following Argentinean institutions: Consejo Nacional de Investigaciones Científicas y Técnicas, Agencia Nacional de Promoción Científica y Tecnológica, and UBACyT from Universidad de Buenos Aires.

[1] A. Schüller, S. Wethekam, and H. Winter, Phys. Rev. Lett. **98**, 016103 (2007).
[2] P. Rousseau, H. Khemliche, A. G. Borisov, and P. Roncin, Phys. Rev. Lett. **98**, 016104 (2007).
[3] H. Winter, Nucl. Instrum. Methods B **332**, 195 (2014).
[4] J. E. Miraglia and M. S. Gravielle, Phys. Rev. A **84**, 062901 (2011).
[5] M. S. Gravielle, J. E. Miraglia, A. Schüller, and H. Winter, Nucl. Instrum. Methods B **317**, 77 (2013)
[6] M. Busch, J. Lienemann, J. Seifert, A. Schuller, and H. Winter, Vacuum **86**, 1618 (2012).
[7] P. Roncin, J. Villette, J. P. Atanas, and H. Khemliche, Phys. Rev. Lett. **83**, 864 (1999).
[8] H. Winter, A. Mertens, S. Lederer, C. Auth, F. Aumayr, and HP. Winter, Nucl. Instrum. Methods B **212**, 45 (2003).
[9] H. Winter, S. Lederer, K. Maass, A. Mertens, F. Aumayr, and HP. Winter, J. Phys. B **35**, 3315 (2002).

[10] C. Auth, A. G. Borisov, and H. Winter, Phys. Rev. Lett. **75**, 2292 (1995).

[11] H. Winter, C. Auth, and A. G. Borisov, Nucl. Instrum. Methods B **115**, 133 (1996).

[12] W. Johnson, free code nrhf.f. The original code needed to be adapted to incorporate also the central potential $V_M(r)$ instead of the nuclear alone.

[13] J. E. Miraglia and M. S. Gravielle (unpublished).

[14] J. E. Miraglia and M. S. Gravielle, Phys. Rev. A **78**, 052705 (2008).

[15] S. Lencinas, J. Burgdörfer, J. Kemmler, O. Heil, K. Kroneberger, N. Keller, H. Rothard, and K. O. Groeneveld, Phys. Rev. A **41**, 1435 (1990).